

Study Method of the P&O Algorithm using Pulse Width Modulation and Duty Cycle Modulation: Application to the search for the Maximum Power Point of PV Systems

Theodore Louossi¹, Kitmo¹, F. N. Gildas Armel², Nanfak Arnaud³, Doka Baza Gilbert¹,

Hamda Marcel Soulouknga⁴, Fatima T. Ahmed⁵

Abstract: In this paper, we make a comparative study of the P&O algorithm using pulse width modulation (PWM) and duty cycle modulation (DCM) for the control of DC/DC converters used for the search of the maximum power point of photovoltaic systems. The converter used here is a boost chopper. Details of the two modulation techniques are presented, and the results are obtained using MATLAB/Simulink software. These results show that the power at the output of the PV oscillates around 0.2W for the DCM technique and 0.6W for the PWM. The output power of the boost chopper shows an oscillation of 0.8W for DCM and 2.4W for PWM. The DCM, in terms of speed reaches the PPM 0.012s less than the PWM. We can therefore say that DCM is better than PWM.

Keywords: PV System, MPPT, Partial shading, Duty cycle modulation, P&O algorithm

History

Received: 30-05-2025;

Revised: 15-08-2025;

Accepted: 28-09-2025



Kitmo, T. Louossi,

kitmobahn@gmail.com

louossitheodore@yahoo.fr

¹Department of Renewable Energy, National Advanced School of Engineering of Maroua, University of Maroua, Maroua, Cameroon

²Laboratory of Energetics and Thermal Applied process (LETA), ENSAI, the University of Ngaoundere P.O. Box 445 ENSAI Ngaoundere, Cameroon

³Department of Energy, Materials, Modelling and Methods, National Higher Polytechnic School of Douala, University of Douala PO Box 2701, Douala-Cameroon

⁴Department of Physics, University of Sarh, Sarh, Chad

⁵Department of Atmospheric Science, College of Science, Mustansiriyah University, Baghdad, Iraq

1. Introduction

Renewable energy is a topical area and is of particular interest to researchers in the field. Today, with the rapid growth of the population, the demand for energy is also becoming very important. Fossil fuels alone cannot meet the demand, which is why renewable energies are being used. There are several types of renewable energy sources, including wind energy using wind power, hydroelectric power using water power, biomass and photovoltaic energy using the sun as a source. The latter has attracted our attention because of its abundant availability. However, the electricity produced by photovoltaic systems depends on environmental conditions such as temperature and solar radiation. These factors affect the current and voltage characteristics of the system, which is why a maximum power point tracking (MPPT) regulator is required to collect the maximum available power [1]. One of the methods used for this is the perturb and observe (P&O) algorithm [2-4]. The perturb and observe algorithm is one of extensively and preferment scheme of maximum power point

tracking algorithm. Like all the different methods used for tracking the maximum power point of photovoltaic system [5-7], perturb and observe method use a pulse width modulation (PWM) for control the DC-DC converter. Here, we propose to use DCM instead of PWM, and then make a comparative study. The DCM is a signal conversion class in which an input signal is converted to a pulse width modulation (PWM). x is transformed to a periodic switching wave $x_m(t)$ with $T_m(x)$ as a period and $R_m(x)$ as a duty cycle. In the literature [8-10] it is shown that this modulation technic offers more advantages than PWM in the field of signal processing. Here it is a question for us to use it in the field of renewable energies for the research of MPP and to compare it with the classically used technic (PWM) [17-19].

For the rest, we organized the work as follows: In section 2, we will present the configuration of the PV system used for the study. The principles of the PWM and DCM technics will be described in section 3. The simulation results will be presented and the comparison between the two modulation technics will be made in section 4 and concluded in section 5.

2. PV system configuration

Fig. 1 illustrates the conversion chain of a PV system. It consists of the PV array, a DC/DC converter connected to the load, an MPPT controller and an adapter stage located between the controller and the DC/DC converter.

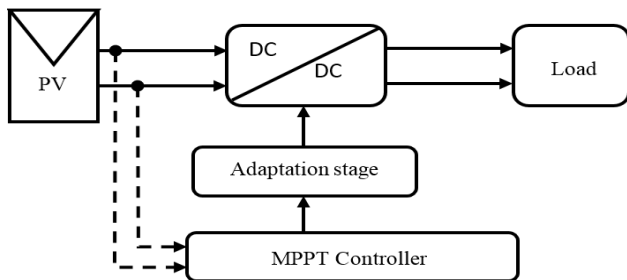


Fig. 1: Configuration of PV power system

2.1 Solar cell and PV module

The operating principle of PV cells is based on the principle of the " photovoltaic effect" [11], which consists of transforming the rays received from the sun or photons into electrical energy. The equivalent circuit of a PV cell is shown in Fig. 2.

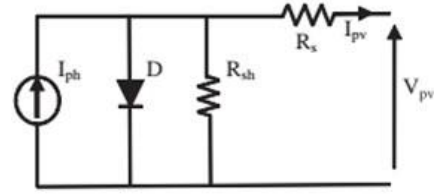


Fig. 2: Equivalent circuit of solar cell

By applying the node law, the output current is calculated as follows I_{pv} given to equation (1)

$$I_{pv} = I_{ph} - I_d - I_{sh} \quad (1)$$

The photo current is proportional to solar irradiation (G in W/m^2) and can be expressed by (2)

$$I_{ph} = \left(\frac{G}{G_r}\right) (I_{scr} + k_i(T - T_r)) \quad (2)$$

Where I_{scr} is short-circuit current of the PV module at standard test condition (STC) of $25^\circ C$ and $1000W/m^2$, k_i is temperature coefficient of short-circuit, T is cell temperature (K) T_r is reference temperature (K) and G_r is reference solar irradiation (W/m^2). The diode current is given by (3)

$$I_d = I_s \left(\exp\left(\frac{q(V_{pv} + R_s I_{pv})}{nK_b T}\right) - 1 \right) \quad (3)$$

Where I_s is saturation current and can be expressed by equation (4), q is electron's charge, n is ideality factor and K_b is Boltzmann's constant.

$$I_s = I_{rs} \left(\frac{T}{T_r}\right)^3 \exp\left(\frac{qE_g}{nK_b} \left(\frac{1}{T_r} - \frac{1}{T}\right)\right) \quad (4)$$

Where I_{rs} is saturation current at T_r and is given by equation (5), E_g is the silicon gap energy of the semiconductor,

$$I_{rs} = \frac{I_{scr}}{\exp\left(\frac{qV_{oc}}{nK_b T}\right) - 1} \quad (5)$$

Where V_{oc} is the open-circuit voltage. The shunt current is given by equation (6),

$$I_{sh} = \frac{V_{pv} + R_s I_{pv}}{R_{sh}} \quad (6)$$

For N_s cells in series and N_p cells in parallel, the characteristic equation of a PV module is delivered as below (7)

$$I_{pv} = N_p I_{ph} - N_p I_s \left(\exp \left(\frac{q(V_{pv} + R_s I_{pv})}{N_s n K_b T} \right) - 1 \right) - \frac{V_{pv} + R_s I_{pv}}{R_{sh}} \quad (7)$$

2.2 DC/DC power Converter

The converter used here is a boost type chopper. It is used to convert direct current from one voltage level to another. It is one of the most widely used converters in the field of renewable energies because of its advantages [12]. Its circuit is shown in Fig. 3.

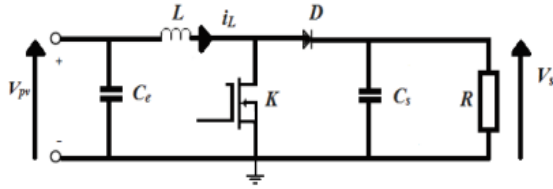


Fig. 3: DC/DC boost converter

The input voltage is V_e which is also the voltage coming out of the PV cell so $V_e = V_{pv}$ and V_s is the output voltage and is expressed as (8)

$$V_s = \frac{V_{pv}}{1-D} \quad (8)$$

The K-switch used in these systems is usually an IGBT or MOSFET [5]. The passive components R, L, C_c and

C_s are respectively the resistance which is the load, the inductance, the input and output capacitors.

2.3 P&O MPPT algorithm

It is one of the most widely used algorithms because of its ease of implementation [13]. As its name suggests, it works on the idea of introducing a disturbance at the operating point in order to observe maximum power at the output. Its principle consists of disturbing the voltage of the PV array while acting on the duty cycle α . Following this disturbance, the power is calculated at a time k then compare to the previous one ($n - 1$). If the power increases, it means that we are approaching the PPM, if not, we are moving away from the PPM if the power decreases at the output of the panel. The summary of this algorithm is given as follows and Fig. 4, illustrates the flowchart of this algorithm: First, the voltage $V_{pv}(n)$ and current $I_{pv}(n)$ are measured for calculating the power $P_{pv}(n)$. The variations of power $\Delta P_{pv} = P_{pv}(n) - P_{pv}(n - 1)$ and of voltage $\Delta V_{pv} = V_{pv}(n) - V_{pv}(n - 1)$ are calculated. If $\Delta P_{pv} \times \Delta V_{pv} > 0$, the duty cycle $\alpha(n + 1) = \alpha(n) + \Delta\alpha$, If $\Delta P_{pv} \times \Delta V_{pv} < 0$, the duty cycle $\alpha(n + 1) = \alpha(n) - \Delta\alpha$.

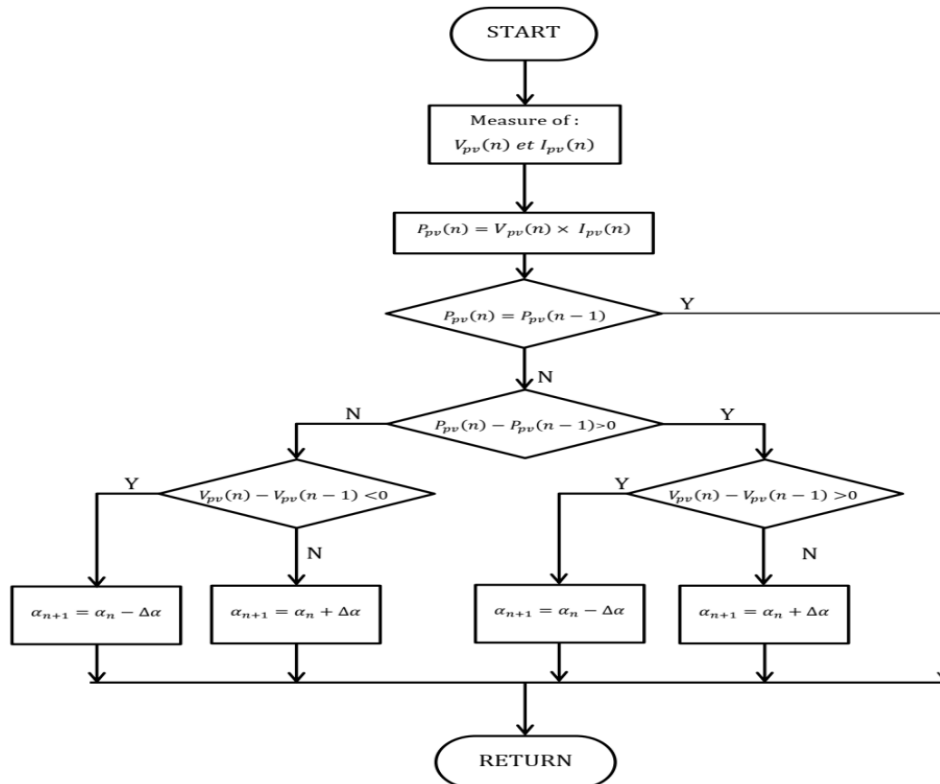


Fig. 4: P&O algorithm [5]

3. Modulations techniques

3.1 PWM technique

Pulse width modulation is one of the oldest techniques and is used in PV systems to convert a DC to DC (in the case of choppers) or a DC to AC (in the case of inverters) [14]. The principle of this control is to synthesize sinusoidal signals from DC signals. This technique is based on the comparison of two signals: one is called the reference signal, and the other is called the reference signal. f_m and the other called a carrier f_p . Two parameters characterize this control strategy: the modulation index m and the modulation rate r_p .

3.2 Non Inverting DCM

Duty Cycle Modulation (DCM) is a variable frequency technic. The principle of DCM is that an input signal x is transformed into a periodic switching wave $x_m(t)$ and period $T_m(x)$ and duty cycle $R_m(x)$. The circuit in Fig. 5, illustrates the DCM circuit proposed in [15]. It consists of an operational amplifier (OPA) combined with four passive components (resistors).

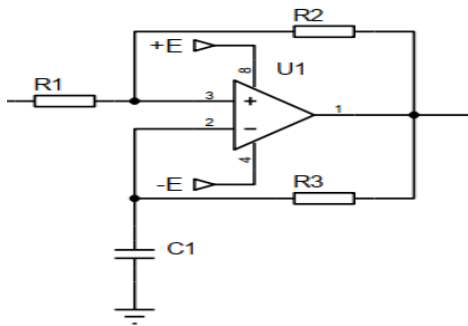


Fig. 5: Non inverting duty cycle modulation [16]

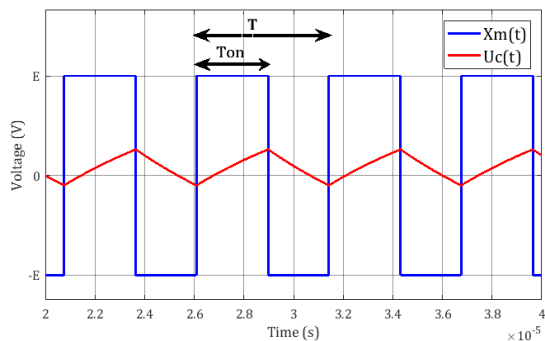


Fig. 6: Steady state of a non-inverting DCM with a constant control

The output signal of non-inverting DCM $x_m(t)$ is a periodic switching wave with period T_m and pulse width T_{on} depend on the control signal x . The signal obtained for a constant control is shown in Fig. 6.

The period T_m and pulse width T_{on} can be computed as follows,

$$T_{on}(x) = \tau \ln \left(\frac{\alpha_2 x - (1 - \alpha_1) V_{sat}}{\alpha_2 x + (\alpha_1 - 1) V_{sat}} \right)$$

and

$$T_m(x) = \tau \ln \left(\frac{(\alpha_2 x)^2 - ((1 + \alpha_1) V_{sat})^2}{(\alpha_2 x)^2 - ((\alpha_1 - 1) V_{sat})^2} \right)$$

where

$$\tau = RC, \alpha_1 = \frac{R_1}{R_1 + R_2} \text{ and } \alpha_2 = 1 - \alpha_1$$

Thus, the resulting duty-cycle is given by

$$R_m(x) = \frac{T_{on}(x)}{T_m(x)} = \frac{\ln \left(\frac{\alpha_2 x - (1 - \alpha_1) V_{sat}}{\alpha_2 x + (\alpha_1 - 1) V_{sat}} \right)}{\ln \left(\frac{(\alpha_2 x)^2 - ((1 + \alpha_1) V_{sat})^2}{(\alpha_2 x)^2 - ((\alpha_1 - 1) V_{sat})^2} \right)}$$

The Fig. 7 and Fig. 8 shows the evolution of the Duty Cycle and frequency as a function of the control voltage for different resistance values R_2 .

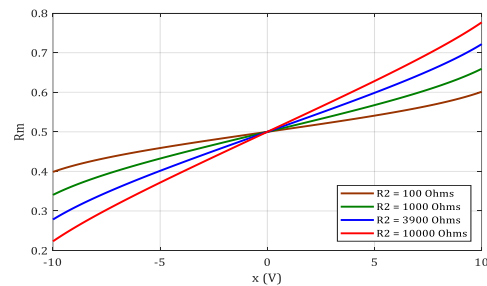


Fig. 7: Duty-cycle of a non inverting DCM

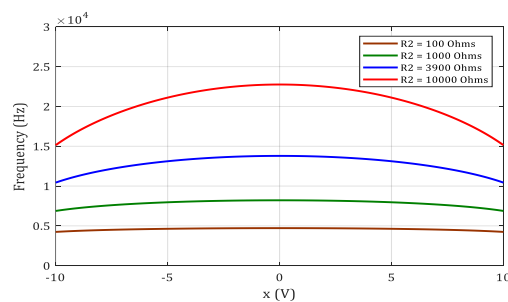


Fig. 8: Frequency of a non-inverting DCM

In addition to its simple and high quality structure, the DCM has a spectral signature that is less rich in harmonics than that of a PWM signal [8-9].

4. Simulation Results

The results of comparison between P&O MPPT algorithm using the PWM technic and the DCM technic for PV system operated under standard environmental conditions (25°C and 1000 W/m^2), under variable irradiation and under variable temperatures are presented. In this work, Matlab Simulink tool is used for simulations. The parameters of the boost converter, P&O MPPT algorithm and the Specification of the PV module are listed in [16].

Fig. 9 to Fig. 12 represent I-V and P-V characteristics with different solar radiations (250 W/m^2 , 500 W/m^2 , 750 W/m^2 and 1000 W/m^2) and a constant ambient temperature fixed at 25°C . Fig. 9 & Fig. 10 represent I-V and P-V characteristics with different ambient temperatures (0°C , 25°C , 50°C and 75°C) and a constant solar radiation fixed at 1000 W/m^2 . The power output characteristic of PV system is nonlinear and crucially influenced by solar radiation and temperature as it is shown.

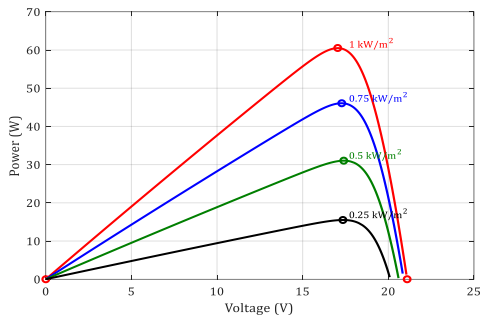


Fig. 9: P-V characteristic at different solar radiations

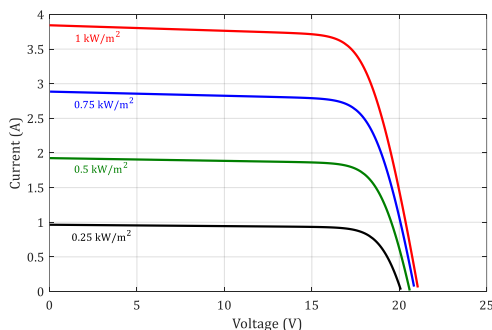


Fig. 10: I-V characteristic at different solar radiations

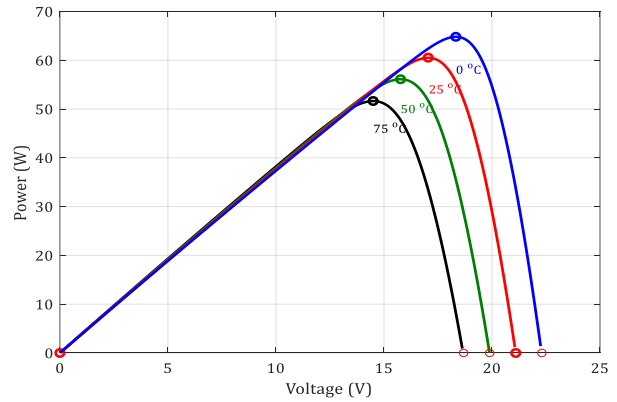


Fig. 11: P-V characteristic at different ambient temperatures

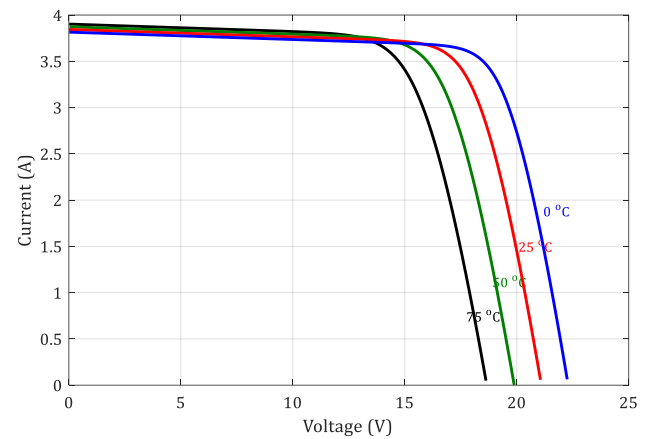


Fig. 12: P-V characteristic at different ambient temperatures

The switching frequency of PWM generator is 10 kHz. The Fig. 13 to Fig. 21 shows the power of PV module (Fig. 13, 16 and 19), the output power of boost converter (Fig. 14, 17 and 20) and duty cycle (Fig. 15, 18 and 21) for PWM and DCM.

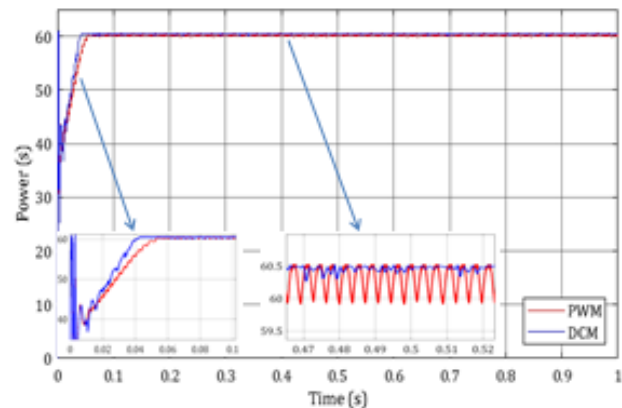


Fig. 13: Power of PV module for standard environmental conditions

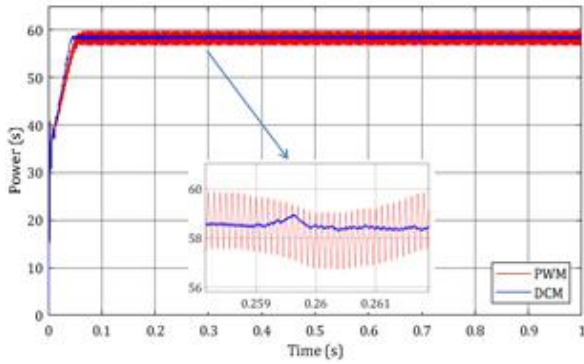


Fig. 14: Output power of Boost converter for standard environmental conditions

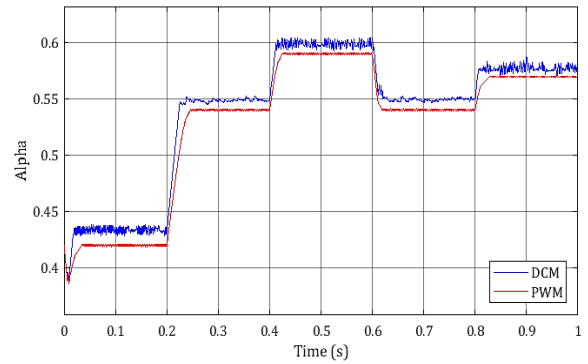


Fig. 18: Duty cycle for constant temperature and varying irradiation

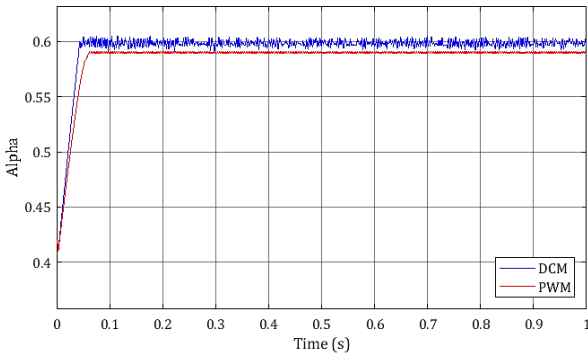


Fig. 15: Duty cycle for standard environmental conditions

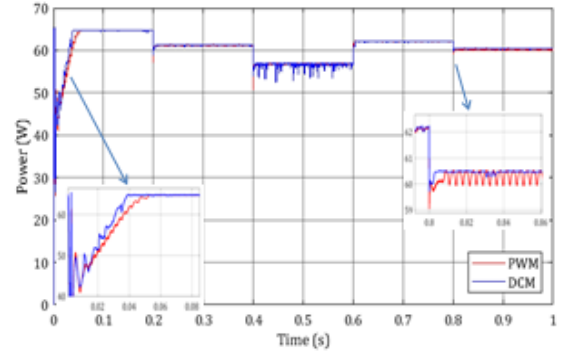


Fig. 19: Power of PV module for constant irradiation and varying temperature

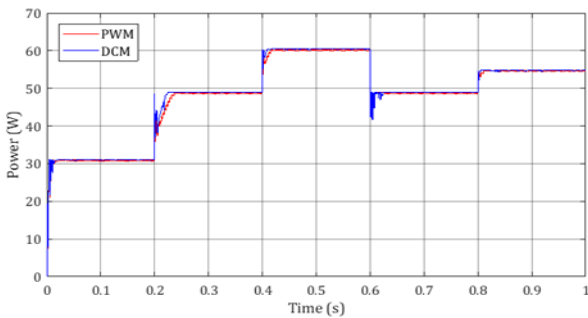


Fig. 16: Power of PV module for constant temperature and varying irradiation

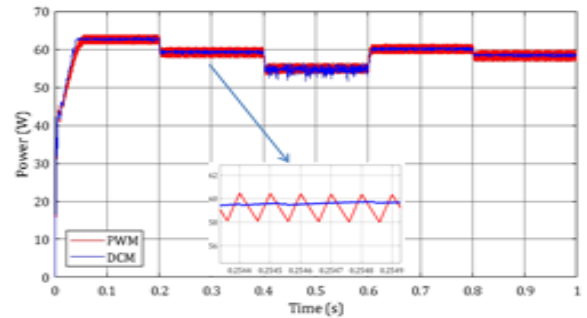


Fig. 20: Output power of Boost converter for constant irradiation

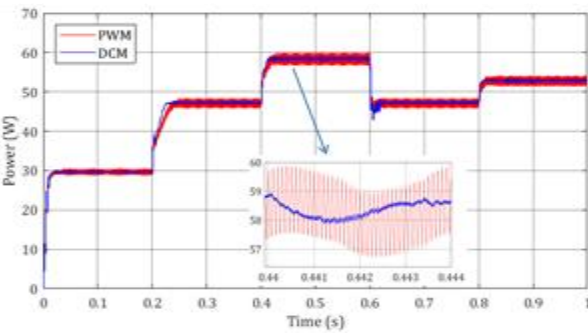


Fig. 17: Output power of Boost converter for constant temperature and varying irradiation

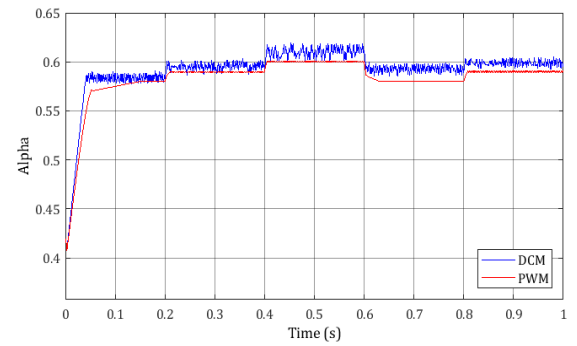


Fig. 21: Duty cycle for constant irradiation and varying temperature

Table 1: Comparison between DCM and PWM

	Modulation techniques	Oscillations	Rise time to reach PPM
Power at the output PV system	DCM	0.2W	0.04s
	PWM	0.6W	0.052s
Power at the output of the Boost chopper	DCM	0.8W	0.04s
	PWM	2.4W	0.052s

The comparison between the P&O algorithm using DCM and the one using PWM to track de MPP is giving in the Table. 1. The results obtained for different climatic variations show that: The power at the output of the PV has an oscillation of 0.2W, at the output of the chopper 0.8W for the DCM. On the other hand, with PWM, the power at the output of the PV is evaluated at 2.4W. The MPP is reached from 0.04s for the DCM and 0.052s for the PWM. From these results, we can say that the DCM has less oscillation and reaches the MPP faster than the PWM.

5. Conclusion

Two approaches of P&O MPPT technic are presented in this paper to track MPP of PV system under different temperatures and different irradiations. The first approach uses pulse width modulation while the second approach uses duty-cycle modulation to control the DC-DC converter. Based on the simulation results obtained with Matlab/Simulink, the dynamic and steady state performance of the P&O MPPT algorithm using duty-cycle modulation is better than that using pulse width modulation.

Conflict of Interest

Authors declared "No conflict of interest".

References

- [1] T. Louossi, N. Djongyang, O. T. S. Mayi, A. Nanfak "Perturb and observe maximum power point tracking method for photovoltaic systems using duty cycle modulation", *Journal of Renewable Energies*, Vol. 23, No. 2, pp. 159-175, 2020.
<https://doi.org/10.54966/jreen.v23i2.41>
- [2] F. Yonga, C. Welba, T. Louossi, N. Djongyang "A New Control Approach of a Three Phase Inverter Two Levels", *Open Journal of Energy Efficiency*, Vol. 11, No. 3, pp. 55-70, 2022.
<http://dx.doi.org/10.4236/ojee.2022.113005>
- [3] F. E. Tahiri, K. Chikh, M. Khafallah, A. Saad "Comparative study between two Maximum Power Point Tracking techniques for photovoltaic system", *2016 International Conference on Electrical and Information Technologies (ICEIT)*, pp. 107 - 112, 2016.
<https://doi.org/10.1109/EITech.2016.7519571>
- [4] E. G. Meena and N. A. Elkhateeb "Enhancing photovoltaic MPPT with P&O algorithm performance based on adaptive PID control using exponential forgetting recursive least squares method", *Renewable Energy*, Vol. 237, art. no. 121801, 2024.
<https://doi.org/10.1016/j.renene.2024.121801>
- [5] R. Khanaki, M. A. M. Radzi, M. H. Marhaban "Comparison of ANN and P&O MPPT methods for PV applications under changing solar irradiation", *2013 IEEE Conference on Clean Energy and Technology (CEAT)*, pp. 287-292, 2013.
<https://doi.org/10.1109/CEAT.2013.6775642>
- [6] A. Kchaou, A. Naamane, Y. Koubaa, N. K. M'Sirdi, "Comparative study of different MPPT techniques for a stand-alone PV system", *2016 17th International Conference on Sciences and Techniques of Automatic Control and Computer Engineering (STA)*, pp. 629-634, 2016.
<https://doi.org/10.1109/STA.2016.7952092>
- [7] R. Kumar, B. Kumar, D. Swaroop "Fuzzy Logic based Improved P&O MPPT Technique for Partial Shading Conditions", *2018 International Conference on Computing, Power and Communication Technologies (GUCON)*, pp. 775-779, 2018.
<https://doi.org/10.1109/GUCON.2018.8674917>
- [8] E. N. P. Lionnel, A. O. Biyobo, P. O. Etouke, Y. P. D. Sounsoumou, R. J. J. Molu, and S. R. D. Naoussi "Modeling and virtual simulation of the boost chopper by DCM using the optimal

- PIDF control", *Heliyon*, Vol. 10, No. 12, art. no. e32657, 2024.
<https://doi.org/10.1016/j.heliyon.2024.e32657>
- [9] A. Obono Biyobo, N. Leandre, Nneme, et J. Mbihi, "A Novel Sine Duty-Cycle Modulation Control Scheme for Photovoltaic Single-Phase Power Inverters", *WSEAS Transactions on Circuits and Systems*, Vol. 17, pp. 105-113, 2018. [Cross Ref]
- [10] S. Salman, X. Ai, and Z. Wu "Design of a P-&-O algorithm based MPPT charge controller for a stand-alone 200W PV system", *Protection and control of modern power systems*, Vol. 3, No. 1, pp. 1-8, 2018.
<https://doi.org/10.1186/s41601-018-0099-8>
- [11] F. N. G. Armel, B. Jacques, et al., "Numerical characterization of solar radiation applied to a simplified five parameters diode model of a photovoltaic module in the city of Ngaoundere", *International Journal of Engineering & Technology*, Vol. 13, No. 1, pp. 132-139, 2024.
<http://dx.doi.org/10.14419/2zb55s42>
- [12] J. K. Udavalakshmi, M. S. Sheik "Comparative Study of Perturb & Observe and Look-Up Table Maximum Power Point Tracking Techniques using MATLAB Simulink", *2018 International Conference on Current Trends towards Converging Technologies (ICCTCT)*, Coimbatore, pp. 1-5, 2018.
<https://doi.org/10.1109/ICCTCT.2018.8550835>
- [13] N. Drir, L. Barazane, M. Loudini "Comparative study of maximum power point tracking methods of photovoltaic systems", *IEEE Transactions on Sustainable Energy*, Vol. 4, No. 1, pp. 89-98, 2013.
<https://doi.org/10.1109/TSTE.2012.2202294>
- [14] A. Z. Arsad, A. W. M. Zuhdi, A. D. Azhar, C. F. Chau, and A. Ghazali. "Advancements in maximum power point tracking for solar charge controllers", *Renewable and Sustainable Energy Reviews*, Vol. 210, art. no. 115208, 2025.
<https://doi.org/10.1016/j.rser.2024.115208>
- [15] L. N. Nneme, J. Mbihi., "Modeling and Simulation of a New Duty-Cycle Modulation Scheme for Signal Transmission Systems", *American Journal of Electrical Electronic Engineering*, Vol. 2, No. 3, pp. 82-87, 2014.
<http://dx.doi.org/10.12691/ajeee-2-3-4>
- [16] T. Louossi, F. K. Mbakop, A. Adje, N. Djongyang "Modeling of an electrical energy switching system in multisource power plants: the case of grid connected photovoltaic and wind power systems", *Journal of Renewable Energy*, Vol. 2022, art. no. 9972334, 2022.
<https://doi.org/10.1155/2022/9972334>
- [17] P. A. Duvalier, B. Jacques, J. B. Bidias, T. Louossi, D. B. Gilbert, K. K. Dieudonne, J. L. Nsouandele, N. Djongyang, and C. Kapseu "A Robust Maximum Power Point Tracking Control under Shading Effects on Photovoltaic Systems", *International Transactions on Electrical Engineering and Computer Science*, Vol. 4, No. 3, pp. 137-151, 2025.
<https://doi.org/10.62760/iteecs.4.3.2025.144>
- [18] Yaouba, M. Bajaj, C. Welba, K. Bernard, Kitmo, S. Kamel, and M. F. El-Naggar "An experimental and case study on the evaluation of the partial shading impact on PV module performance operating under the sudano-sahelian climate of Cameroon", *Frontiers in Energy Research*, Vol. 10, art. no. 924285, 2022.
<https://doi.org/10.3389/fenrg.2022.924285>
- [19] Kitmo, G. B. Tchaya, and N. Djongyang "Optimization of the photovoltaic systems on the North Cameroon interconnected electrical grid", *International Journal of Energy and Environmental Engineering*, Vol. 13, No. 1, pp. 305-317, 2022.
<https://doi.org/10.1007/s40095-021-00427-8>



Copyright: © 2025 by the authors, Licensee ITEECS, India. This article is an open access article distributed under the terms and conditions of the Creative Commons Attribution (CC BY) license (<https://creativecommons.org/licenses/by/4.0/>).
